Extent computation under rank-deficient conditions

Alma Mašić [*] **Julien Billeter** [**] **Dominique Bonvin** [**]
Kris Villez [*]

[*] *Eawag: Swiss Federal Institute of Aquatic Science and Technology,*
Überlandstrasse 133, CH-8600 Dübendorf, Switzerland
[**] *Laboratoire d'Automatique, École Polytechnique Fédérale de*
Lausanne, CH-1015 Lausanne, Switzerland

Abstract: The identification of kinetic models can be simplified via the computation of extents of reaction on the basis of invariants such as stoichiometric balances. In the extent space, one can identify the structure and the parameters of reaction rates individually, which significantly reduces the number of parameters that need to be estimated simultaneously. So far, extent-based modeling has only been applied to cases where all the extents can be computed from measured concentrations. This generally excludes its application to many biological processes for which the number of reactions tends to be larger than the number of measured quantities. This paper shows that, in some cases, such restrictions can be lifted. In addition, this study demonstrates the applicability of extent-based model identification using laboratory experimental data.

Keywords: biotechnology, environmental engineering, extents, model identification, resource recovery, urine nitrification, wastewater treatment

1. INTRODUCTION

The computation of extents of reaction from measured concentrations has been advocated as a way of simplifying the modeling task for complex reaction systems. With extents, one can turn the joint estimation of all rate laws and kinetic parameters into smaller estimation problems involving a single reaction at the time (Bhatt et al., 2011). This divide-and-conquer approach allows reducing the computational complexity of finding appropriate rate laws (Mašić et al., 2016a; Srinivasan et al., 2016). This is similar to the problem studied in Kotte and Heinemann (2009). However, the solution of Kotte and Heinemann (2009) assumes steady state conditions and a just determined or underdetermined nature of the parameter estimation problem. Neither of these assumptions are necessary to apply the extent-based framework. To this day, extent-based model identification is limited to cases where there are at least as many measured concentrations as there are reactions, which clearly limits the applicability of this method to reaction systems with a sufficient number of measurements. This generally excludes biological wastewater-treatment processes. This work illustrates that the computation of some but not all extents is possible and applies this for extent-based modeling.

2. MATERIALS AND METHODS

2.1 Problem statement

We demonstrate the developed method by means of data collected during a single cycle (a batch) of an intermittently fed stirred-tank reactor for biological urine nitrification (Udert and Wächter, 2012; Fumasoli et al., 2016).

This cycle starts with a short feeding of source-separated urine collected at Eawag with No-Mix toilets (Larsen et al., 2001). During this cycle, ammonia is oxidized to nitrite by ammonia oxidizing bacteria (AOB) and the produced nitrite is oxidized to nitrate by nitrite oxidizing bacteria (NOB). The aim of this experiment is to estimate a dynamic model describing the growth and decay of both AOB and NOB. Ammonia and nitrite are measured with Hach Lange cuvette tests approximately every 30 minutes during the considered cycle, leading to 29 samples.
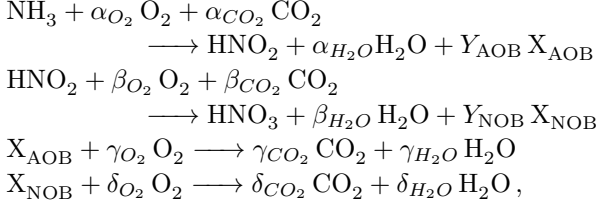
2.2 Process model

Theory. The process can be modeled as a set of ordinary differential equations (ODEs):

$$\dot{\boldsymbol{c}}(t) = \mathbf{N}^{\mathrm{T}}\,\boldsymbol{r}\big(\boldsymbol{c}(t), \boldsymbol{\theta}\big), \quad \boldsymbol{y}_h = \mathbf{G}\,\boldsymbol{c}(t_h), \qquad \boldsymbol{c}(0) = \boldsymbol{c}_0 \quad (1)$$

$$\tilde{\boldsymbol{y}}_h = \boldsymbol{y}_h + \boldsymbol{\epsilon}_h \qquad \boldsymbol{\epsilon}_h \sim \mathcal{N}(\mathbf{0}, \boldsymbol{\Sigma}_h)\,, \qquad (2)$$

with $\boldsymbol{c}$ the S-dimensional concentration vector, $\boldsymbol{r}$ the R-dimensional vector of reaction rates, $\mathbf{N}$ the $R \times S$ stoichiometric matrix, $\tilde{\boldsymbol{y}}$ the M-dimensional measurement vector, $\mathbf{G}$ the $M \times S$ measurement gain matrix, where M denotes the number of measured quantities, $\boldsymbol{\epsilon}$ the measurement error vector, $\boldsymbol{\Sigma}$ the measurement error variance-covariance matrix, and h the sampling index ($h = 1, 2, \ldots, H$). The structures of the rate laws $\boldsymbol{r}\big(\boldsymbol{c}(t), \boldsymbol{\theta}\big)$ are assumed to be known, but not the parameters $\boldsymbol{\theta}$. One also assumes that $\boldsymbol{c}_0$ is known and the parameters $\boldsymbol{\theta}$ are structurally identifiable (as in Dochain et al., 1995; Petersen et al., 2003) or otherwise known.

Application. The process is described by a two-step nitrification model involving two growth processes and two decay processes:

$$NH_3 + \alpha_{O_2}\,O_2 + \alpha_{CO_2}\,CO_2$$
$$\longrightarrow HNO_2 + \alpha_{H_2O}H_2O + Y_{AOB}\,X_{AOB}$$
$$HNO_2 + \beta_{O_2}\,O_2 + \beta_{CO_2}\,CO_2$$
$$\longrightarrow HNO_3 + \beta_{H_2O}\,H_2O + Y_{NOB}\,X_{NOB}$$
$$X_{AOB} + \gamma_{O_2}\,O_2 \longrightarrow \gamma_{CO_2}\,CO_2 + \gamma_{H_2O}\,H_2O$$
$$X_{NOB} + \delta_{O_2}\,O_2 \longrightarrow \delta_{CO_2}\,CO_2 + \delta_{H_2O}\,H_2O\,,$$

with X_{AOB} and X_{NOB} the AOB and NOB biomasses, and Y_{AOB} and Y_{NOB} the yield coefficients of AOB and NOB. The internalization of nitrogen into the biomass is ignored. The growth processes are modeled with two Monod-type reaction rates while the decay processes are described with first-order kinetics. We assume a stable pH and express all rates as functions of component concentrations (e.g. total ammonia, total nitrite). In the considered model, the concentrations of CO_2, H_2O, and O_2 do not affect the reaction rates. As they are not measured either, they are omitted from the model. The model is defined with:

$$c = \begin{bmatrix} c_{TAN} & c_{TNO_2} & c_{TNO_3} & c_{AOB} & c_{NOB} \end{bmatrix}^T \tag{3}$$

$$G = \begin{bmatrix} 1 & 0 & 0 & 0 & 0 \\ 0 & 1 & 0 & 0 & 0 \end{bmatrix} \tag{4}$$

$$N = \begin{bmatrix} -1 & 1 & 0 & Y_{AOB} & 0 \\ 0 & -1 & 1 & 0 & Y_{NOB} \\ 0 & 0 & 0 & -1 & 0 \\ 0 & 0 & 0 & 0 & -1 \end{bmatrix} \tag{5}$$

$$r = \begin{bmatrix} \mu_{AOB}\,c_{AOB}\,c_{TAN}/(K_{AOB} + c_{TAN}) \\ \mu_{NOB}\,c_{NOB}\,c_{TNO_2}/(K_{NOB} + c_{TNO_2}) \\ b_{AOB}\,c_{AOB} \\ b_{NOB}\,c_{NOB} \end{bmatrix}\,, \tag{6}$$

where c_{TAN}, c_{TNO_2}, c_{TNO_3}, c_{AOB}, and c_{NOB} are the total ammonia, total nitrite, total nitrate, AOB, and NOB concentrations. The matrix G indicates that the concentrations of ammonia and nitrite are measured. The stoichiometric matrix N includes the unknown yield coefficients Y_{AOB} and Y_{NOB}. The kinetic parameters are the maximum specific growth rates (μ_{AOB}, μ_{NOB}), the affinity constants (K_{AOB}, K_{NOB}), and the specific decay rates (b_{AOB}, b_{NOB}).

Define the relative biomass concentrations z_{AOB} and z_{NOB}:

$$z_{AOB}(t) = c_{AOB}(t)/c_{AOB,0} \tag{7}$$
$$z_{NOB}(t) = c_{NOB}(t)/c_{NOB,0}\,, \tag{8}$$

with $c_{AOB,0} = c_{AOB}(0)$ and $c_{NOB,0} = c_{NOB}(0)$.

The specific growth rate parameters (μ_{AOB}, μ_{NOB}) and the yields (Y_{AOB}, Y_{NOB}) are replaced by the new parameters

$$a_{AOB} = \mu_{AOB}\,c_{AOB,0}/Y_{AOB},\quad n_{AOB} = Y_{AOB}/c_{AOB,0} \tag{9}$$
$$a_{NOB} = \mu_{NOB}\,c_{NOB,0}/Y_{NOB},\quad n_{NOB} = Y_{NOB}/c_{NOB,0}. \tag{10}$$

The equivalent concentration vector, stoichiometric matrix, and rate vector are:

$$c \leftarrow \begin{bmatrix} c_{TAN} & c_{TNO_2} & c_{TNO_3} & z_{AOB} & z_{NOB} \end{bmatrix}^T \tag{11}$$

$$N \leftarrow \begin{bmatrix} -1 & 1 & 0 & n_{AOB} & 0 \\ 0 & -1 & 1 & 0 & n_{NOB} \\ 0 & 0 & 0 & -1 & 0 \\ 0 & 0 & 0 & 0 & -1 \end{bmatrix} \tag{12}$$

$$r \leftarrow \begin{bmatrix} a_{AOB}\,z_{AOB}\,c_{TAN}/(K_{AOB} + c_{TAN}) \\ a_{NOB}\,z_{NOB}\,c_{TNO_2}/(K_{NOB} + c_{TNO_2}) \\ b_{AOB}\,z_{AOB} \\ b_{NOB}\,z_{NOB} \end{bmatrix}\,, \tag{13}$$

with all remaining equations as in (1)-(4) and the symbol $\leftarrow$ indicating a redefinition. In the remainder, the redefined vector c includes the inorganic nitrogen concentrations in their original scale and the biomass concentrations in their relative scale. The relative biomass concentrations (z_{AOB}, z_{NOB}) are further referred to as the biomass concentrations unless specified otherwise. The model exhibits 8 parameters (a_{AOB}, b_{AOB}, n_{AOB}, K_{AOB}, a_{NOB}, b_{NOB}, n_{NOB}, and K_{NOB}) that are unknown and need to be estimated.

2.3 Definition of extents of reaction

As in previous work, the extents of reaction x indicate the cumulative progress of the reactions, measured in moles, since the start of the experiment. One writes:

$$x(t) = x_0 + V \int_0^t r(c(\tau))d\tau\,, \tag{14}$$

with V the known and constant reactor volume. Importantly, this definition means that the concentrations can be expressed as functions of the extents:

$$c(t) = c_0 + N^T\,\frac{x(t)}{V}. \tag{15}$$

2.4 Computation of extents under rank-deficient conditions

For the case with at least as many measured species as independent reactions, Rodrigues et al. (2015) showed how to compute the extents by means of a linear transformation. With rank(N)$=R$, this transformation requires rank($G\,N^T$)$=R$, from which it follows that $M \geq R$. If the number of measurements is such that $M < R$, it is no longer possible to compute all R extents from M measurements without a kinetic model. In addition, the $M \times R$ matrix $G\,N^T$ can be rank deficient. Let $A := \text{rank}(G\,N^T)$, with $A \leq M < R$.

Theory. The idea in this work is to compute a reduced number of extents, say the R^o *observable extents* $x^o(t)$, from the M measurements $y(t) = G\,c(t)$, with $R^o < R$. For this purpose, we propose to construct the $R^o \times R$ selection matrix S to select R^o observable extents among the R extents, $x^o = S\,x$. S can be constructed as follows:

- Rearrange the matrix $G\,N^T$ in *reduced row echelon form* via Gauss-Jordan elimination (Meyer, 2000)
- Remove the rows that contain a zero vector and the rows that contain more than one non-zero element to generate the matrix S. The number of rows in S is $R^o \leq A$.

In what follows, we consider the case $R^o = A$. When so, $S^T S$ is an $R \times R$ diagonal matrix with R^o ones and $(R - R^o)$ zeros on the diagonal. The zeros on the diagonal correspond to columns in $G\,N^T$ that are zero vectors, which allows writing $G\,N^T S^T S = G\,N^T$. It follows that $G\,N^T x = G\,N^T S^T x^o$, and thus

$$y_h = G\left(c_0 + N^T x(t_h)/V\right)$$
$$= G\left(c_0 + N^T S^T x^o(t_h)/V\right). \tag{16}$$

With this selection of observable extents, one can find a unique solution to the extent computation problem, which is quadratic in the extents:

$$\hat{\boldsymbol{x}}_h^{\mathrm{o}} = \arg\min_{\boldsymbol{x}_h^{\mathrm{o}}} \sum_{h=1}^{H} \left(\tilde{\boldsymbol{y}}_h - \boldsymbol{y}_h\right)^{\mathrm{T}} \boldsymbol{\Sigma}_h^{-1} \left(\tilde{\boldsymbol{y}}_h - \boldsymbol{y}_h\right) \qquad (17)$$

$$\text{s.t.} \quad \boldsymbol{y}_h = \mathbf{G}\left(\boldsymbol{c}_0 + \mathbf{N}^{\mathrm{T}} \mathbf{S}^{\mathrm{T}} \boldsymbol{x}_h^{\mathrm{o}}/V\right). \qquad (18)$$

The estimates $\hat{\boldsymbol{x}}_h^{\mathrm{o}}$ ($h = 1,\ldots,H$) are referred to as *experimental observable extents*.

Application. Let us discuss the construction of the matrix $\mathbf{S}$ for the example introduced above, with $S = 5$, $R = 4$, and $M = 2$. The matrix $\mathbf{G}\,\mathbf{N}^{\mathrm{T}}$ is

$$\mathbf{G}\,\mathbf{N}^{\mathrm{T}} = \begin{bmatrix} -1 & 0 & 0 & 0 \\ 1 & -1 & 0 & 0 \end{bmatrix}, \qquad (19)$$

with the following reduced row echelon form:

$$(\mathbf{G}\,\mathbf{N}^{\mathrm{T}})_{rref} = \begin{bmatrix} 1 & 0 & 0 & 0 \\ 0 & 1 & 0 & 0 \end{bmatrix}. \qquad (20)$$

As $(\mathbf{G}\,\mathbf{N}^{\mathrm{T}})_{rref}$ has no rows with only zeros or more than one non-zero element, $\mathbf{S} = (\mathbf{G}\,\mathbf{N}^{\mathrm{T}})_{rref}$. The $R^{\mathrm{o}} = 2$ observable extents correspond to the growth reactions. The extents of the two decay reactions cannot be observed on the basis of the stoichiometric balances.

2.5 Reconstructed concentrations

Theory. Given the extents $\boldsymbol{x}(t)$, one can always reconstruct the concentration vector using (15). However, for the case $R^{\mathrm{o}} < R$, there are $R^{\mathrm{u}} = R - R^{\mathrm{o}}$ unobservable extents labeled $\boldsymbol{x}^{\mathrm{u}}$. Hence, one can only reconstruct the concentrations for the species that do not involve these unobservable extents. The $R \times S$ stoichiometric matrix $\mathbf{N}$ can be partitioned into the $R^{\mathrm{o}} \times S$ submatrix $\mathbf{N}^{\mathrm{o}}$ corresponding to the observable reactions and the $R^{\mathrm{u}} \times S$ submatrix $\mathbf{N}^{\mathrm{u}}$ corresponding to the unobservable reactions, $\mathbf{N} = \begin{bmatrix} \mathbf{N}^{\mathrm{o}} \\ \mathbf{N}^{\mathrm{u}} \end{bmatrix}$. Eq. (15) can be written as:

$$\boldsymbol{c}(t) = \boldsymbol{c}_0 + 1/V\left(\mathbf{N}^{\mathrm{o}\mathrm{T}}\boldsymbol{x}^{\mathrm{o}} + \mathbf{N}^{\mathrm{u}\mathrm{T}}\boldsymbol{x}^{\mathrm{u}}\right). \qquad (21)$$

All the species with a column in $\mathbf{N}^{\mathrm{u}}$ that contains at least one non-zero element are affected by the unobservable reactions and, thus, cannot be reconstructed solely from the observable experimental extents $\hat{\boldsymbol{x}}_h^{\mathrm{o}}$. These concentrations are labeled as *structurally unobservable*, similarly to Kretsovalis and Mah (1987). Among the remaining unlabeled species, one then finds those species whose columns in $\mathbf{N}^{\mathrm{o}}$ contain only known stoichiometric parameters. These concentrations are labeled as *structurally observable* since the effect of the observable extents on these concentrations is known and there are no effects of unobservable extents. The remaining unlabeled concentrations are also labeled as *structurally unobservable*. The number of structurally observable concentrations is S^{o} and their concentration vector is $\boldsymbol{c}^{\mathrm{o}}$. Note that this observability consideration is based on the stoichiometric balance alone. It does not account for the use of a dynamic model to estimate unmeasured concentrations given that the parameter of the dynamic model are not available yet. The following procedure can be used to identify the structurally observable concentrations:

Given the above labeling, the matrix $\mathbf{R}$ is constructed as an $S^{\mathrm{o}} \times S$ matrix with a single one in every row and zeros elsewhere. Each row in $\mathbf{R}$ corresponds to a structurally observable species. The position of the element 1 identifies the species. Hence, one can write, $\boldsymbol{c}^{\mathrm{o}} := \mathbf{R}\,\boldsymbol{c}$. With this, the observable concentration estimates are:

$$\hat{\boldsymbol{c}}_h^{\mathrm{o}} = \mathbf{R}\left(\boldsymbol{c}_0 + \mathbf{N}^{\mathrm{T}}\mathbf{S}^{\mathrm{T}}\hat{\boldsymbol{x}}_h^{\mathrm{o}}/V\right). \qquad (22)$$

Application. The identification of structurally observable concentrations is illustrated with the example introduced above. The matrix $\mathbf{N}$ is partitioned as follows:

$$\mathbf{N}^{\mathrm{o}} = \begin{bmatrix} -1 & 1 & 0 & n_{\mathrm{AOB}} & 0 \\ 0 & -1 & 1 & 0 & n_{\mathrm{NOB}} \end{bmatrix}$$

$$\mathbf{N}^{\mathrm{u}} = \begin{bmatrix} 0 & 0 & 0 & -1 & 0 \\ 0 & 0 & 0 & 0 & -1 \end{bmatrix}. \qquad (23)$$

In the matrix $\mathbf{N}^{\mathrm{u}}$, one observes non-zero elements in the columns corresponding to the concentrations z_{AOB} and z_{NOB}. Hence, these concentrations are unobservable. Since the first three columns of $\mathbf{N}^{\mathrm{o}}$, corresponding to the unlabeled concentrations c_{TAN}, c_{TNO_2}, and c_{TNO_3}, contain only known stoichiometric parameters, the concentrations c_{TAN}, c_{TNO_2}, and c_{TNO_3} are observable. It follows that $S^{\mathrm{o}} = 3$ and that the 3×5 matrix $\mathbf{R}$ reads:

$$\mathbf{R} = \begin{bmatrix} 1 & 0 & 0 & 0 & 0 \\ 0 & 1 & 0 & 0 & 0 \\ 0 & 0 & 1 & 0 & 0 \end{bmatrix}. \qquad (24)$$

2.6 Subsystem identification

In previous work on kinetic identification, every extent was modeled individually, with the other extents needed to compute the reaction rates being interpolated from experimental measurements. This is no longer possible here as there are extents for which no value can be computed. Hence, a slightly different approach is taken by identifying the smallest subsets of reactions whose kinetic parameters can be estimated separately from all other reactions. The main difference with previous work is that these subsystems may include more than a single reaction.

Theory. A graph-based algorithm is used to determine the smallest subsystems whose parameters can be identified separately. An introduction to graph theory is available in Deo (2004). Here, we use directed bipartite graphs with two sets of nodes corresponding to extents and concentrations. The arcs from extents to concentrations represent the algebraic relationships (15) used for reconstruction. The arcs from concentrations to extents represent the integration of the differential equations (14). Nodes representing the interpolated extents are called *interpolation nodes*. All the remaining nodes are referred to as *variable nodes* and represent concentrations and extents that are simulated dynamically during parameter estimation. Each of the graphs ($\mathcal{G}_v, v = 1,\ldots,V$) identified with the following algorithm represents a subsystem whose parameters are estimated together:

(1) Create a graph $\mathcal{G}_0$ with nodes for all concentrations and extents defined in (14) and (15).
(2) For each non-zero stoichiometric element $\mathbf{N}_{r,c}$ in $\mathbf{N}$, add a directed arc to $\mathcal{G}_0$ from the extent r to the concentration c. This reflects the structure of (15).
(3) Among the directed arcs in the graph, label the arcs that link the computed extents to the concentrations that can be reconstructed as *reconstruction* arcs. These arcs correspond to elements of $\mathbf{N}$ that are retained in $\mathbf{S}\,\mathbf{N}\,\mathbf{R}^{\mathrm{T}}$ and reflects the structure in (22).

(4) A directed arc is added to $\mathcal{G}_0$ from every concentration appearing in a rate law to the extent of that reaction. This reflects the rate law structures in (1).

(5) Remove all reconstruction arcs.

(6) Remove all single-node components.

(7) Identify the connected components in the graph and index them with v ($1 \leq v \leq V$). Set $v = 1$.

(8) Define $\mathcal{G}_v$ as the vth connected component in $\mathcal{G}_0$.

(9) Add those arcs removed from $\mathcal{G}_0$ in Step (5) that have at least their ending node in $\mathcal{G}_v$. Add the starting nodes of these arcs in $\mathcal{G}_0$ if they are not already in $\mathcal{G}_v$.

(10) Identify the strongly connected components in $\mathcal{G}_v$. Label the nodes not included in any strongly connected component as an *interpolation node*. All remaining nodes are labeled as a *variable node*.

(11) If $v < V$, set $v \leftarrow v+1$ and go to (7). Else, terminate.

Application. The graphs generated for the illustrative example are shown in Fig. 1. Fig. 1a shows the graph $\mathcal{G}_0$ obtained at Step (3) of the algorithm. This graph represents the relationships involved when simulating the complete system. The rightward arcs represent the computation of concentrations on the basis of extents. One sees that knowing z_{AOB} requires knowledge of x_1 and x_3, while knowing z_{NOB} requires knowledge of x_2 and x_4. Similarly, knowing c_{TAN} (c_{TNO_2}; c_{TNO_3}) requires x_1 (x_1 and x_2; x_2). The leftward arcs represent the structure of the rate laws used to simulate the extents (14). c_{TAN} appears only in the AOB growth rate law (cf. x_1) and c_{TNO_2} appears only in the NOB growth rate law (cf. x_2). c_{TNO_3} appears in none of the rate laws. z_{AOB} appears in the AOB growth and decay rate laws (cf. x_1 and x_3). Finally, z_{NOB} appears in the NOB growth and decay rate laws (cf. x_2 and x_4).

The dashed arcs represent the possibility to obtain a number of concentrations via reconstruction on the basis of the experimental extents (22). As established before, this is possible for c_{TAN}, c_{TNO_2}, and c_{TNO_3}. In Step (5) these arcs are removed. As a result, the graph is split in three components. One component has the nodes x_1, x_3, c_{TAN}, and z_{AOB}. A second component has the nodes x_2, x_4, c_{TNO_2}, and z_{NOB}. The last component is the single-node component with node c_{TNO_3}. This third component is removed in Step (6) so that only the first two components remain in Step (7) ($V = 2$). This completes $\mathcal{G}_0$.

Steps (8) to (10) lead to the graph $\mathcal{G}_1$ shown in Fig. 1b corresponding to the first component in $\mathcal{G}_0$. In Step (9), the arc from x_1 to c_{TAN} in $\mathcal{G}_0$ is added to $\mathcal{G}_1$. There are no further arcs to add. In addition, the re-introduced arc has all of its nodes in $\mathcal{G}_1$ already so that no nodes are added. In Step (10) one identifies a single strongly connected component in $\mathcal{G}_1$ consisting of all nodes and all arcs. All nodes are part of a strongly connected component. Consequently, there are no interpolation nodes. This means that identifying the kinetic parameters involved in the identified subsystem does not require interpolation. Simulation of the $\mathcal{G}_1$ subsystem involves the parameters a_1, b_1, n_1, and K_1.

Steps (8) to (10) are now repeated for the second component in $\mathcal{G}_0$. The result is shown in Fig. 1c. In this case, two arcs in $\mathcal{G}_0$ are introduced into $\mathcal{G}_2$: from x_1 to c_{TNO_2}
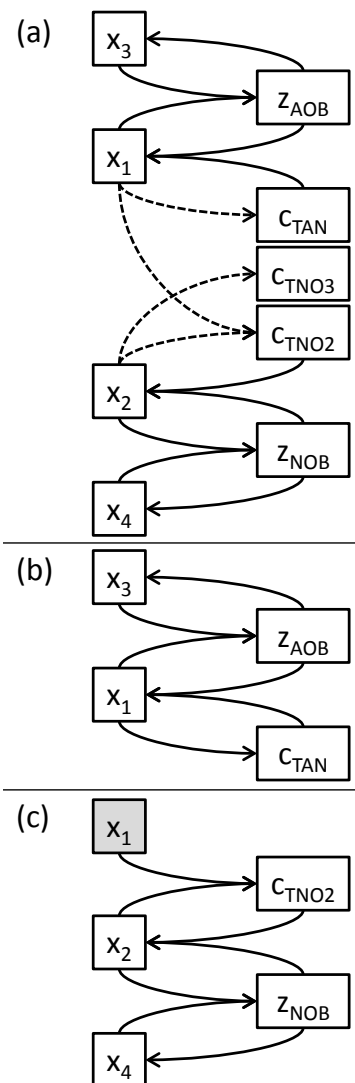

Fig. 1. Graphs obtained during subsystem identification at Step (4) (subplot a) and at Step (11) (subplots b and c). Dashed arcs indicate interpolation arcs. Grey shading of nodes indicates the interpolation nodes.

and from x_2 to c_{TNO_2}. x_1 is added as a node as it does not appear in $\mathcal{G}_2$ initially. Again, Step (10) leads to the identification of a single strongly connected component. This time it consists of the nodes x_2, x_4, c_{TNO_2}, and z_{NOB} and all arcs between these nodes. The node x_1 is not in the strongly connected component and thus is an interpolation node. This means that the interpolated first experimental extent ($\hat{x}_1$) is used as a known input to simulate the subsystem represented by $\mathcal{G}_2$. Such simulations involve the parameters a_2, b_2, n_2, and K_2.

2.7 Parameter estimation

Following the identification of each subsystem, all stoichiometric and kinetic parameters involved in the simulation are estimated jointly. In this work, we adopt the deterministic optimization method given in Mašić et al. (2016b).

3. RESULTS

3.1 Experimental data

The top panel of Fig. 2 shows the $H = 29$ measurements of ammonia and nitrite concentrations ($\tilde{y}_h$) as a function of time (t_h) within the considered process cycle. One can see that the ammonia concentration decreases from about 70 to 0 g/m³ as a consequence of the AOB activity. As a result, the nitrite concentration initially increases from 0 to a maximum of 20 g/m³ at 5 h, after which it decreases again to zero. This indicates that the nitrite oxidization process is slower than the ammonia oxidation process. We assume that the measurement errors are uncorrelated and exhibit a standard deviation of 5% of the measured values.

3.2 Extent computation

The experimental extents computed by means of (17)-(18) are shown in Figs. 3 and 4 as a function of time. The profiles suggest a monotonic progress of the growth reactions and illustrate the slower progress of the nitrite oxidation compared to the ammonia oxidation.
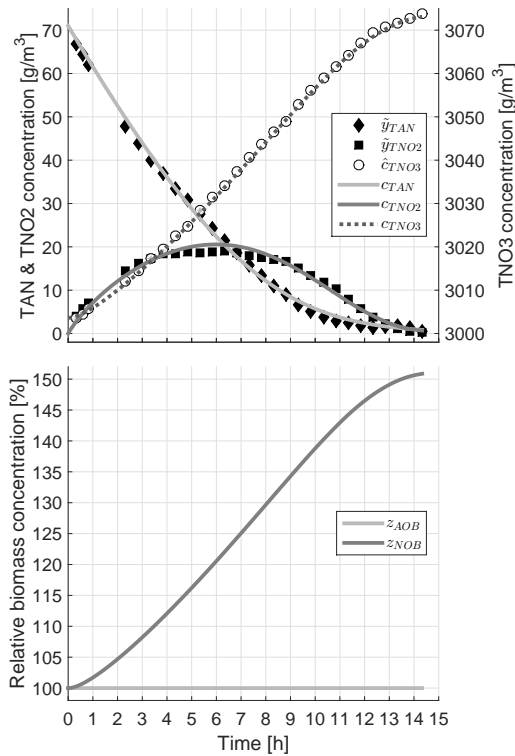

Fig. 2. Concentrations as a function of time during a single cycle of intermittently fed biological urine nitrification process. *Top:* Ammonia and nitrite concentration measurements ($\tilde{y}_{TAN}$, $\tilde{y}_{TNO2}$), nitrate concentration estimates ($\hat{c}_{TNO3}$), and simulated ammonia, nitrite, and nitrate concentrations with the complete model (c_{TAN}, c_{TNO2}, c_{TNO3}). *Bottom:* Simulated relative biomass concentrations with the complete model.

3.3 Reconstructed concentrations

The nitrate concentration $\hat{c}_{TNO3}$ can be reconstructed from the experimental extents using (22). In the top panel of Fig. 2, one sees that these estimates follow the sigmoid profile of the extent of the NOB growth reaction in Fig. 4.

3.4 Parameter estimation

Parameter estimation is executed for each of the two subsystems identified in Section 2.6. This means that the parameters a_1, b_1, n_1, and K_1 are optimized so that the extent of the AOB growth reaction simulated with Subsystem 1 (Fig. 1b) best matches the first extent in the weighted least-squares (WLS) sense. Similarly, the parameters a_2, b_2, n_2, and K_2 are adjusted in a second optimization so that the extent of the NOB growth reaction best matches the second extent, also in the WLS sense. Figs. 3 and 4 show that the identified subsystem models approximate the experimental extents well.

3.5 Recombined model

The identified parameters are used to simulate the complete system (1)-(4) with (12)-(13). The ammonia, nitrite, and nitrate concentrations obtained by means of this simulation are shown in the top panel of Fig. 2. One sees that the modeled concentrations approximate the measured and estimated concentrations well. The simulated
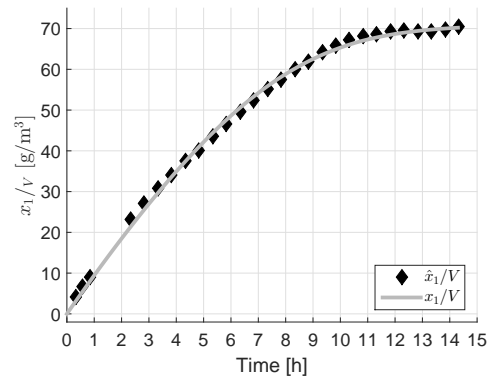

Fig. 3. Extent of AOB growth as a function of time: (◆) measurements, (——) model prediction.
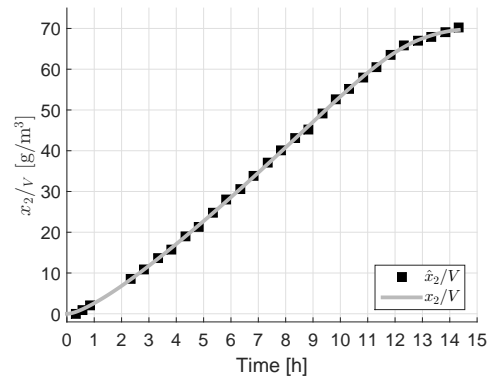

Fig. 4. Extent of NOB growth as a function of time: (■) measurements, (——) model prediction.

relative biomass concentrations are shown in the bottom panel of Fig. 2. One sees that identified model parameters suggest that the net AOB growth is marginal while the NOB underwent a 50% increase during the experiment.

4. DISCUSSION

4.1 Benefits of the method

This contribution has presented a first case of extent-based modeling under rank-deficient conditions. Prior work has claimed that the stoichiometric matrix $\mathbf{N}^{\mathrm{T}}$ or – in case of unmeasured species – the matrix $\mathbf{G}\,\mathbf{N}^{\mathrm{T}}$ must be of rank R to enable extent computation and modeling of the individual extents. This is true if one assumes that computing the extent of every reaction is necessary. However, one may still be able to compute a smaller number of extents of reaction if the rank condition is not satisfied. In addition, one may also be able to divide the parameter estimation problem into smaller problems involving only parameters affecting the dynamics of the computed extents. Both claims were illustrated using data obtained from a biological urine nitrification process. Extent computation allows reducing the size of parameter sets that need to be identified simultaneously, thus leading to an increased efficiency of the model identification process – this despite not satisfying rank conditions that were considered essential previously.

A serendipitous benefit of the modeling method is that it leads to a reformulation of the model, whereby the yield coefficients become lumped into the parameters of the kinetic rate laws. As a consequence, one does not need to know the yield coefficients to describe the measured concentrations.

4.2 Opportunities and future work

It was shown for one case that the matrix $\mathbf{G}\,\mathbf{N}^{\mathrm{T}}$ does not need to be full rank to benefit from the extent-based modeling philosophy. However, it remains to be evaluated how general this situation is. The currently imposed requirement that $R^{\mathrm{o}}{=}A$ means that all parameters still need to be estimated simultaneously as soon as $R^{\mathrm{o}} \leq A$. This may still restrict the utility of extent-based model identification in practice and deserves further attention. Even more important, it is relevant to know which variables ought to be measured to separate the model identification task into smaller problems.

5. CONCLUSIONS

Historically, extent-based modeling has been considered applicable to process modeling only when there are at least as many measured variables as there are independent reactions. This contribution demonstrates that this is not a strict requirement for separated estimation of smaller subsets of kinetic parameters. This proves especially valuable for biological systems, where the number of modeled reactions may easily exceed the number of measured variables. In addition, our work demonstrates that model reformulation may allow applying extent-based modeling also when some elements of the stoichiometric matrix are unknown. This strongly benefits the application of extent computation and extent-based modeling to biological systems where the yield coefficients appearing in stoichiometric matrices are typically unknown.

REFERENCES

Bhatt, N., Amrhein, M., and Bonvin, D. (2011). Incremental identification of reaction and mass-transfer kinetics using the concept of extents. *Industrial & Engineering Chemistry Research*, 50(23), 12960–12974.

Deo, N. (2004). *Graph Theory with Applications to Engineering and Computer Science*. PHI Learning Pvt. Ltd.

Dochain, D., Vanrolleghem, P.A., and Van Daele, M. (1995). Structural identifiability of biokinetic models of activated sludge respiration. *Water Research*, 29, 2571–2578.

Fumasoli, A., Etter, B., Sterkele, B., Morgenroth, E., and Udert, K.M. (2016). Operating a pilot-scale nitrification/distillation plant for complete nutrient recovery from urine. *Water Science and Technology*, 73(1), 215–222.

Kotte, O. and Heinemann, M. (2009). A divide-and-conquer approach to analyze underdetermined biochemical models. *Bioinformatics*, 25(4), 519–525.

Kretsovalis, A. and Mah, R.S.H. (1987). Observability and redundancy classification in multicomponent process networks. *AIChE Journal*, 33(1), 70–82.

Larsen, T.A., Peters, I., Alder, A., Eggen, R., Maurer, M., and Muncke, J. (2001). Re-engineering the toilet for sustainable wastewater management. *Environmental Science and Technology*, 35(9), 192A–197A.

Mašić, A., Srinivasan, S., Billeter, J., Bonvin, D., and Villez, K. (2016a). Biokinetic model identification via extents of reaction. In *5th IWA/WEF Wastewater Treatment Modelling Seminar (WWTmod2016), Annecy, France, April 2-6, 2016, appeared on USB-stick.*

Mašić, A., Udert, K., and Villez, K. (2016b). Global parameter optimization for biokinetic modeling of simple batch experiments. *Environmental Modelling and Software*, 85, 356–373.

Meyer, C.D. (2000). *Matrix Analysis and Applied Linear Algebra*. SIAM, Philadelphia, PA.

Petersen, B., Gernaey, K., Devisscher, M., Dochain, D., and Vanrolleghem, P.A. (2003). A simplified method to assess structurally identifiable parameters in Monod-based activated sludge models. *Water Research*, 37(12), 2893–2904.

Rodrigues, D., Srinivasan, S., Billeter, J., and Bonvin, D. (2015). Variant and invariant states for chemical reaction systems. *Computers & Chemical Engineering*, 73, 23–33.

Srinivasan, S., Billeter, J., and Bonvin, D. (2016). Identification of multiphase reaction systems with instantaneous equilibria. *Industrial & Engineering Chemistry Research*, 29(55), 8034–8045.

Udert, K.M. and Wächter, M. (2012). Complete nutrient recovery from source-separated urine by nitrification and distillation. *Water Research*, 46(2), 453–464.